Photo darkening of rare earth doped silica

Mattsson, Kent Erik

Published in:
Optics Express

Link to article, DOI:
10.1364/OE.19.019797

Publication date:
2011

Document Version
Publisher's PDF, also known as Version of record

Photo darkening of rare earth doped silica

Kent E. Mattsson

NKT Photonics A/S, Blokken 84, DK-3460 Birkerød, Denmark / DTU Fotonik, Department of Photonics Engineering, Technical University of Denmark, Ørsteds Plads 343, DK-2800 Kgs. Lyngby, Denmark
KEEM@fotonik.dtu.dk

Abstract: The photo darkening (PD) absorption spectra from unseeded amplifier operation (by 915 nm pumping) of ytterbium / aluminum and co-doped silica fibers is after prolonged operation observed to develop a characteristic line at 2.6 eV (477 nm). This line is proposed to be due to inter center excitation transfer from type II oxygen deficiency centers ODC(II) to Tm^{3+} trace impurities. The ODC(II) is proposed to be the result of a displacive transition of a 4-fold silica ring hosting two 3-fold silicon units that presents two non-bridging oxygen to Yb^{3+} (as part of its 6-fold coordination by oxygen). The displacive transition is initiated by a charge disproportionation process which leads to NBO transfer in forming dioxasilirane (2-fold coordinated silicon with two NBO attached) next to silylene (2-fold coordinated silicon with a lone electron pair). In collaboration with a valence electron of Yb^{3+} a new ½ / 1½ chemical bond is formed on dioxasilirane which comprises the PD color center for the visible and near-infrared. Difference in solid acidity of the silica material co-doped with Yb/Al and Yb/P may explain the observed difference in spectral shapes by change of bond order to the formed chemical bond.

OCIS codes: (060.2290) Fiber materials; (060.2320) Fiber optics amplifiers and oscillators.

References and links

1. J. J. Koponen, M. J. Söderlund, H. J. Hoffman, and S. K. T. Tammela, "Measuring photodarkening from single-mode ytterbium doped silica fibers," Opt. Express **14**(24), 11539–11544 (2006).
2. S. Jetschke, S. Unger, U. Röpke, and J. Kirchhof, "Photodarkening in Yb doped fibers: experimental evidence of equilibrium states depending on the pump power," Opt. Express **15**(22), 14838–14843 (2007).
3. S. Jetschke, S. Unger, A. Schwuchow, M. Leich, and J. Kirchhof, "Efficient Yb laser fibers with low photodarkening by optimization of the core composition," Opt. Express **16**(20), 15540–15545 (2008).
4. S. Yoo, C. Basu, A. J. Boyland, C. Sones, J. Nilsson, J. K. Sahu, and D. Payne, "Photodarkening in Yb-doped aluminosilicate fibers induced by 488 nm irradiation," Opt. Lett. **32**(12), 1626–1628 (2007).
5. M. Engholm and L. Norin, "Preventing photodarkening in ytterbium-doped high power fiber lasers; correlation to the UV-transparency of the core glass," Opt. Express **16**(2), 1260–1268 (2008).
6. J. Jasapara, M. Andrejco, D. DiGiovanni, and R. Windeler, "Effect of heat and H_2 gas on the photo-darkening of Yb^{+3} fibers," in *Conference on Lasers and Electro-Optics/Quantum Electronics and Laser Science Conference and Photonic Applications Systems Technologies*, Technical Digest (CD) (Optical Society of America, 2006), paper CTuQ5.
7. L. Skuja, "Optically active oxygen-deficiency-related centers in amorphous silicon dioxide," J. Non-Cryst. Solids **239**(1-3), 16–48 (1998).
8. D. L. Griscom, "Trapped-electron centers in pure and doped glassy silica: A review and synthesis," J. Non-Cryst. Solids **357**(8-9), 1945–1962 (2011).
9. D. P. Partlow and A. J. Cohen, "Optical studies of biaxial Al-related color centers in smoky quartz," Am. Mineralogist **71**, 589–598 (1986).
10. F. Mady, M. Benabdesselam, and W. Blanc, "Thermoluminescence characterization of traps involved in the photodarkening of ytterbium-doped silica fibers," Opt. Lett. **35**(21), 3541–3543 (2010).
11. C. G. Carlson, K. E. Keister, P. D. Dragic, A. Croteau, and J. G. Eden, "Photoexcitation of Yb-doped aluminosilicate fibers at 250 nm: evidence for excitation transfer from oxygen deficiency centers to Yb^{3+}," J. Opt. Soc. Am. B **27**(10), 2087–2094 (2010).
12. M. J. Söderlund, J. J. Montiel i Ponsoda, J. P. Koplow, and S. Honkanen, "Heat-induced darkening and spectral broadening in photodarkened ytterbium-doped fiber under thermal cycling," Opt. Express **17**(12), 9940–9946 (2009).

#150869 - $15.00 USD Received 11 Jul 2011; revised 2 Sep 2011; accepted 2 Sep 2011; published 26 Sep 2011

13. J. K. Sahu, S. Yoo, A. J. Boyland, C. Basu, M. P. Kalita, A. Webb, C. L. Sones, J. Nilsson, and D. N. Payne, "488 nm irradiation induced photodarkening study of Yb doped aluminosilicate and phosphosilicate fibers," in *Conference on Lasers and Electro-Optics/Quantum Electronics and Laser Science Conference and Photonic Applications Systems Technologies*, OSA Technical Digest (CD) (Optical Society of America, 2008), paper JTuA27.
14. Y. W. Lee, S. Sinha, M. J. F. Digonnet, R. L. Byer, and S. Jiang, "Measurement of high photodarkening resistance in heavily Yb^{3+}-doped phosphate fibres," Electron. Lett. **44**(1), 14–16 (2008).
15. M. Engholm, P. Jelger, F. Laurell, and L. Norin, "Improved photodarkening resistivity in ytterbium-doped fiber lasers by cerium codoping," Opt. Lett. **34**(8), 1285–1287 (2009).
16. K. E. Mattsson, "Low photo darkening single mode RMO fiber," Opt. Express **17**(20), 17855–17861 (2009).
17. K. Bogumil, J. Orphal, and J. P. Burrows, "Temperature dependent absorption cross sections of O_3, NO_2, and other atmospheric trace gases measured with the SCIAMACHY spectrometer," Proceeding Envisat Symposium Goteborg, Sweden (2000), http://earth.esa.int/pub/ESA DOC/gothenburg/099bog
18. B. Schaudel, P. Goldner, M. Prassas, and F. Auzel, "Cooperative luminescence as a probe of clustering in Yb^{3+} doped glasses," J. Alloy. Comp. **300–301**(1-2), 443–449 (2000).
19. S. Jetschke, S. Unger, A. Schwuchow, M. Leich, V. Reichel, and J. Kirchhof, "Photodarkening in Yb-doped silica fibers: influence of the atmosphere during perform collapsing," Proc. SPIE **6873**, 68731G, 68731G-10 (2008).
20. L. Skuja, "Direct singlet-to-triplet optical absorption and luminescence excitation band of the twofold-coordinated silicon center in oxygen-deficient glassy SiO_2," J. Non-Cryst. Solids **167**(3), 229–238 (1994).
21. J. T. Fournier and R. H. Bartram, "Inhomogeneous broadening of the optical spectra of Yb^{3+} in phosphate glass," J. Phys. Chem. Solids **31**(12), 2615–2624 (1970).
22. L. Pauling, "The nature of silicon-oxygen bonds," Am. Mineral. **65**, 321–323 (1980).
23. V. O. Sokolov and V. B. Sulimov, "Threefold coordinated oxygen atom in silica glass," J. Non-Cryst. Solids **217**(2-3), 167–172 (1997).
24. S. Jetschke, M. Leich, S. Unger, A. Schwuchow, and J. Kirchhof, "Influence of Tm- or Er-codoping on the photodarkening kinetics in Yb fibers," Opt. Express **19**(15), 14473–14478 (2011).
25. R. Peretti, A.-M. Jurdyc, B. Jacquier, C. Gonnet, A. Pastouret, E. Burov, and O. Cavani, "How do traces of thulium explain photodarkening in Yb doped fibers?" Opt. Express **18**(19), 20455–20460 (2010).
26. K. C. Snyder and W. B. Fowler, "Oxygen vacancy in α -quartz: a possible bi- and metastable defect," Phys. Rev. B Condens. Matter **48**(18), 13238–13243 (1993).
27. F. L. Galeener, "Planar rings in vitreous silica," J. Non-Cryst. Solids **49**(1-3), 53–62 (1982).
28. L. Giordano, P. V. Sushko, G. Pacchioni, and A. L. Shluger, "Electron trapping at point defects on hydroxylated silica surfaces," Phys. Rev. Lett. **99**(13), 136801 (2007).
29. K. Awazu and H. Kawazoe, "O_2 molecules dissolved in synthetic silica glasses and their photochemical reactions induced by ArF excimer laser radiation," J. Appl. Phys. **68**(7), 3584–3591 (1990).
30. C. M. Carbonaro, P. C. Ricci, and A. Anedda, "Thermal quenching properties of ultraviolet emitting centers in mesoporous silica," Phys. Rev. B **76**(12), 125431 (2007).
31. V. A. Radtsig and I. N. Senchenya, "Hydrogenation of the silanone groups $(\equiv Si\text{-}O)_2Si{=}O$. Experimental and quantum-chemical studies," Russ. Chem. Bull. **45**(8), 1849–1856 (1996).
32. P. H. Krupenie, "The spectrum of molecular oxygen," J. Phys. Chem. Ref. Data **1**(2), 423–534 (1972).
33. J. Rolfe, F. R. Lipsett, and W. J. King, "Optical absorption and fluorescence of oxygen in alkali halide crystals," Phys. Rev. **123**(2), 447–454 (1961).
34. R. D. Harcourt, "Pauling "3-electron bonds," "increased-valence," and 6-electron 4-center bonding," J. Am. Chem. Soc. **102**(16), 5195–5201 (1980).
35. G. Busca, "The surface acidity of solid oxides and its characterization by IR spectroscopic methods. An attempt at systematization," Phys. Chem. Chem. Phys. **1**(5), 723–736 (1999).
36. B. Morasse, S. Chatigny, E. Gagnon, C. Hovington, J.-P. Martin, J.-P. de Sandro, "Low photodarkening single cladding ytterbium fibre amplifier," Proc. SPIE, 6453, 6453OH (2007)
37. K. Arai, H. Namikawa, K. Kumata, T. Honda, T. Ishii, and T. Handa, "Aluminum or phosphorus co-doping effects on the fluorescence and structural properties of neodymium-doped silica glass," J. Appl. Phys. **59**(10), 3430–3436 (1986).
38. A. Saitoh, S. Matsuishi, M. Oto, T. Miura, M. Hirano, and H. Hosono, "Elucidation of coordination structure around Ce^{3+} in doped SiO2 glasses using pulsed electron paramagnetic resonance: effect of phosphorus, boron, and phosphorus-boron codoping," Phys. Rev. B **72**(21), 212101 (2005).
39. W. J. Miniscalco, "Erbium-doped glasses for fiber amplifiers for 1500 nm," J. Lightwave Technol. **9**(2), 234–250 (1991).

1. Introduction

The development of InGaAs diode lasers specific to pump erbium doped fiber amplifiers for commercial use in telecommunications industry have made cheap, reliable and steadily increasing pump diode laser power available for the 900–980 nm wavelength range. This again has fueled the development of ytterbium co-doped silica fiber amplifiers/lasers that over

#150869 - $15.00 USD Received 11 Jul 2011; revised 2 Sep 2011; accepted 2 Sep 2011; published 26 Sep 2011

time have shown continuous increasing output power levels now reaching into the kW regime even for single mode operation. Photo darkening (PD) lead, however, to serious performance degradation and lifetime limitation for rare earth (RE) co-doped silica fiber devices and its nature has been extensively studied in literature [1–4]. The PD absorption spectra show spectra with centers in the UV and visible stretching long tails into the near infrared. These color centers give raise to increased thermal load which decreases the laser efficiency. Mitigation of PD is therefore the key to further improvement of the performance and reliability of high power fiber lasers / amplifiers.

The PD of ytterbium co-doped silica is generally described to be the result of a multi-step multi-photon absorption process, where several excited RE ions co-operate to supply energy for capturing electron and holes at different structural defects. Both the nature of these defects and the process of color center formation are, however, still under debate. For Yb co-doped silica the electron supplying defects or PD precursors are in [4] oxygen deficiency centers (ODC) whereas [5] suggest charge-transfer-states (CTS) related to Yb^{2+} formation and [6] propose Yb^{2+} formation by capture of electrons on Yb^{3+} pairs. In [4] the color center become electrons captured at Al^{3+} or Yb^{3+} sites and holes captured in E' type color centers [7]. The nature of the Al^{3+} or Yb^{3+} sites for electron capture is not described further in [4] but may be aluminum-associated trapped-electron centers as described in [8]. In [5] the color centers are holes captured on Al^{3+} in substitute Si^{4+} sites as reported by [9] for smoky quartz. In [6] the reduced gain is due to reduced amount of active Yb^{3+} without further assignment of color centers. In [10] the trap characteristics of Yb/Al co-doped silica are analyzed by thermally stimulated luminescence and it is found that PD involves intrinsic silica hole traps but these are not the main color centers responsible for PD. Characteristic Yb^{3+} luminescence (900 nm to 1050 nm) is observed during thermal activation at all temperatures above 75°C. The Yb^{3+} luminescence is in [11] observed during 235 - 260 nm excitations along with luminescence of a row of intrinsic defects of the silica network. In [11] ODC to E' center conversion is proposed to assume a role for the excitation transfer to Yb^{3+} which may also explain the growth in E' centers observed in [4], however, leaving the color center unassigned.

The induced PD is found to be either partially or fully reversed through temperature annealing [12] or exposure to UV and/or visible light. The latter bleaching is in [5,11] observed to be followed by characteristic Yb^{3+} luminescence. Even partial bleach by the pump power (915 nm) gives this possibility [2]. Reduction of PD is also shown by oxygen [4] and hydrogen [6] loading. Co-doping with phosphorous is in [3,4,13] found to reduce the amount of PD and degradation-free Yb co-doped phosphate fibers is reported in [14]. The co-doping with Cerium is in [15] found to improve the durability of Yb/Al-doped fibers.

In this work it is experimentally found that the PD absorption spectrum grows uniform as function of time and spectral structures at ≈477 nm and ≈558 nm develops after prolonged time of operation in Yb/Al co-doped fibers. These lines are proposed to be due to inter center excitation transfer from type II oxygen deficiency centers ODC(II) to Tm^{3+} and Er^{3+} trace impurities, respectively. The ODC(II) is seen as result of a displacive transition followed by a charge disproportionation process in forming a new chemical bond on anion dioxasilirane next to a 2-fold coordinated silicon cation. Difference in solid acidity of the silica material co-doped with Yb/Al and Yb/P may are taken to explain their difference in spectral shape due to difference in the coordination by silicon to the dioxasilirane.

2. Experimental procedure

The set-up for characterization of the fiber samples is shown in Fig. 1 a). The aim of the set-up is to provide information on the spectral shape of the PD induced color centers at the visible and near infrared wavelengths and their temporal evolution. A 100 W low voltage halogen lamp is used as probe light. The collimated light from the halogen lamp is coupled by a microscope objective into the large core, low NA end of a 4 m long taper fiber. The 400 μm core fiber end is tapered down to 150 μm, supporting a NA up to 0.65 at 950 nm, and this end

#150869 - $15.00 USD Received 11 Jul 2011; revised 2 Sep 2011; accepted 2 Sep 2011; published 26 Sep 2011

is butt-joint coupled to the Yb doped fiber under test. Pump power is provided by three multimode laser diode modules (915 nm) with 105/125 µm, 0.22 NA pigtails spliced onto a standard 7:1 multimode power combiner with a 125 µm, 0.45 NA common port. The common port is butt-joint coupled to the Yb doped fiber under test. The pump power goes to 11 W. Probe light is collected from one of the input ports of the power combiner connected to an optical spectrum analyzer (OSA). The OSA is capable of measuring from 350 nm to 1700 nm.

The test fiber lengths in this study are 20 - 50 cm. To prevent lasing at high inversion levels, the test fibers are angle-cleaved at both ends. The measurement is started with the pumps turned off and performing a broadband reference scan with the OSA. Hereafter, the probe light is blocked by a shutter and the pumps are turned on. After some time, the pumps are turned off, the shutter is opened and a broadband OSA scan is performed. This is repeated 7 times during the first hour of the measurement and hereafter for every one hour for 46 hours. With respect to transmitted probe light, the stability of the set-up is better than 0.2-0.4 dB over 46 hours. The OSA is also used to measure the luminescence spectrum from the test fiber while being pumped. The drift in transmitted power due to shift in the coupling efficiency of the butt-joint gives raise to shift in the background reference. To correct for this the spectra are multiplied by a factor that counters this coupling loss. The fiber surface is cooled by agitated air flow to assure equal temperature conditions for the PD experiments. Inspected by thermal camera at the beginning and at the end of a PD experiment the surface temperature was found to be below 30°C for all experiments.

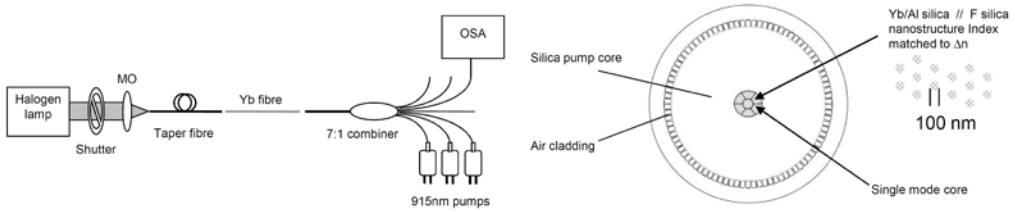

Fig. 1. **a)** Experimental set-up for measurement of PD in unseeded amplifier, **b)** double cladding fiber cross section–single mode core comprising 7 areas surrounded silica pump core and an air clad and outer silica tube protected by a thin polymeric coating (not shown)—the insert show a cross sectional view of the nanostructure silica (index matched to Δn against silica to support single mode operation of the 7 area core) with < 100 nm diameter for the individual rare earth co-doped silica nano-structure islands.

The optical fibers under investigation are of the double core structure where a cross section is illustrated in Fig. 1 b). The core 15 µm–20 µm in diameter comprises 7 sections of nano-structured active material surrounded by a second pump pure silica core of 150 µm diameter and an air cladding for the combined active core / pump core structure as described in [16]. For Yb co-doped silica fibers 6 of 7 sections are Yb/Al nano-structure material embedded in F co-doped silica while the 7th section is germanium co-doped nano-structure material. All sections are matched to same area average refractive index such that the fiber supports single mode operation. For background luminescence and PD reference a fiber with all 7 sections comprising germanium co-doped nanostructure material is applied. For analyzing the influence of nano-structure areas on PD one Yb/Al perform was drawn directly to 15 µm–20 µm core diameter in 150 µm diameter pump silica cores as was the Yb/P co-doped fiber. The two fibers are in the following referred to as uniform core fibers. This work applies six Yb/Al co-doped, one Yb/P co-doped and one pure Ge co-doped fiber. The doping concentrations for fibers #1 - #8 are: #1: 0.63 at % Yb / 2.6 at % Al; #2: 0.73 at % Yb / 2.6 at % Al; #3: 0.08 at % Yb / 0.94 at % Al, #4: 0.34 at % Yb / 2.28 at % Al, #5: 0.14 at % Yb / 0.65 at % Al, #6: 0.26 at % Yb / 2.07 at % Al, #7: 0.09 at % Yb / 3.6 at % P and #8: 6 at % Ge. Fiber #1 to #5 hold 6 of 7 core areas with rare earth co-doping while the 7th area is 6 at % Ge co-doped. Fiber #6 and #7 are uniform core fibers and fiber #8 is a nanostructure fiber with all 7 areas 6 at % Ge co-doped. All atomic concentrations are for total number of

#150869 - $15.00 USD Received 11 Jul 2011; revised 2 Sep 2011; accepted 2 Sep 2011; published 26 Sep 2011

atoms—i.e. Yb per Yb + … + Si + O. The quoted concentrations are the local concentration in the nanostructures that for index matching purpose is emerged in F co-doped silica.

3. Experimental results

In Fig. 2 a) representative absorption spectra obtained for fibers #1 and #2 of high local Yb concentration are shown after 46 hours PD operation with 46% population inversion.

The measured absorption spectra show strong absorption at ≈400 nm with a shoulder at ≈600 nm and a long tail stretching into the near infrared. All recorded Yb/Al spectra (uniform core and nano-structure fibers) develop over time uniformly without observable structural changes except for a dip at 470 nm–480 nm. This is taken to show that the spectrum is the result of absorption by one color center complex. The absorption spectrum of (1 atm 0.26 mol) ozone [17] is shown below the two spectra for comparison. The shoulder and tail of the PD data are observed to follow a spectral distribution similar to ozone. Solid squares of Fig. 2 a) fits the spectra of one uniform core fiber #6 with 0.26 at %, and nano-structure fibers #5: 0.14 at % and #3: 0.08 at % Yb respectively as shown in Fig. 2 b). The three upper curves are spectra of the fibers operated at 46% population inversion whereas the final two spectra are for 35% and 22% population inversion of fiber #3. The tails of the PD spectra scale both with ytterbium concentration and population inversion level.

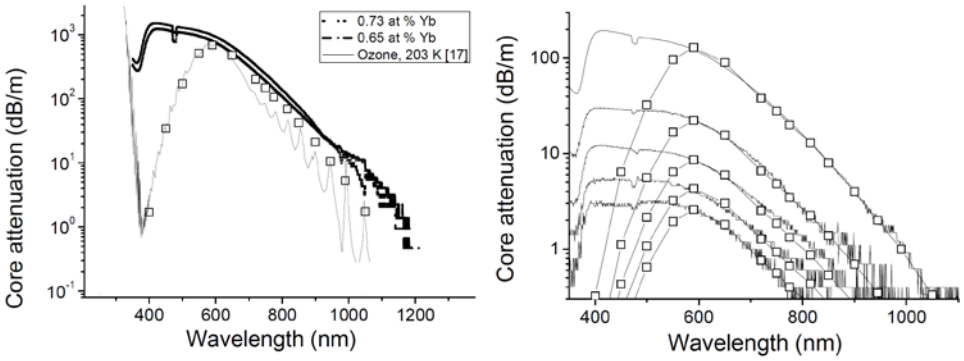

Fig. 2. **a)** PD absorption spectra for 0.63 and 0.7 at % Yb (Al co-doped) fibers together with 1 atm. 0.26 mol O_3 absorption spectrum, **b)** PD absorption spectra of Yb/Al co-doped fibers superimposed "O_3 absorption". The three lowest spectra are for fiber #3 at three different population inversion levels.

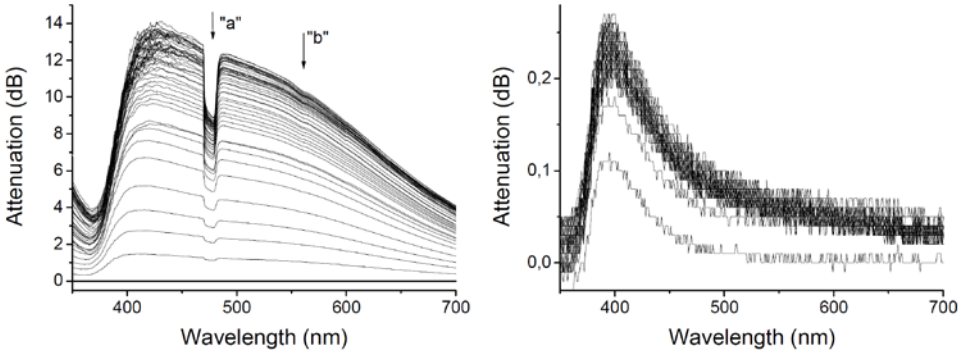

Fig. 3. **a)** PD absorption spectra for fiber #6 (Yb/Al co-doped) uniform core fiber with attenuation growing as function of time, where arrow "a" indicate the 470 nm–480 nm dip and a second feature at "b" being visible as function of time, **b)** PD absorption spectra of Yb/P co-doped fiber showing weak absorption signal without observable 470 nm - 480 nm or 558 nm dips.

#150869 - $15.00 USD Received 11 Jul 2011; revised 2 Sep 2011; accepted 2 Sep 2011; published 26 Sep 2011

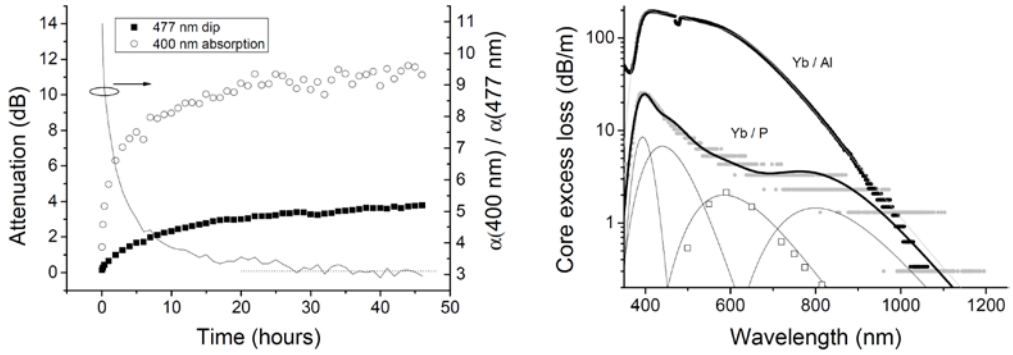

Fig. 4. **a)** PD absorption at 400 nm and 477 nm (dip depth) as function of time along with their ratio as function of time, **b)** PD core spectra for Yb/Al and Yb/P co-doped silica show considerable difference in the visible and comparable absorption in the near infrared. The two spectra can be decomposed by the four Gaussian centers shown—here one is O_3 absorption as indicated by the open squares.

The dip observed in all Al co-doped spectra at 470 nm–480 nm grows as function of time as shown in Fig. 3 a) for a Yb/Al co-doped uniform core material. Along with the dip indicated by the arrow marked "a" a second dent become visible around 558 nm marked by "b" while the slight structure that may be anticipated at 600 nm is an artifact of register change in the OSA. Similar dent is to be observed at the 976 nm (but is not shown in Fig. 3). The spectra of Yb/P co-doped material is shown in Fig. 3 b). Here the features observed in Yb/Al co-doped material are absent (or not resolved) in the much weaker absorption.

The growth in dip (missing 477 nm absorption α(477 nm) relative to the mean α(468 nm) and α(486 nm)) is shown in Fig. 4 a) as function of time along with α(400 nm). By dividing α(400 nm) with α (477 nm) a constant ratio of ≈3.1 is observed after 30 hours.

In Fig. 4 b) typical absorption spectra of all measured Yb/Al and Yb/P co-doped fibers are shown. From Fig. 4 b) it is to be observed that the Yb/P and Yb/Al co-doped fibers follow different distributions, however, the two distributions may be described by nearly identical absorption centers. Here the "ozone" absorption is described by a Gaussian center at 2.12 eV with full width half maximum (FWHM) 0.68 eV. The "remaining" absorption of Yb/Al co-doped material is described by Gaussian centers at 3.12 eV (0.35 eV) and 2.75 eV (0.70 eV).

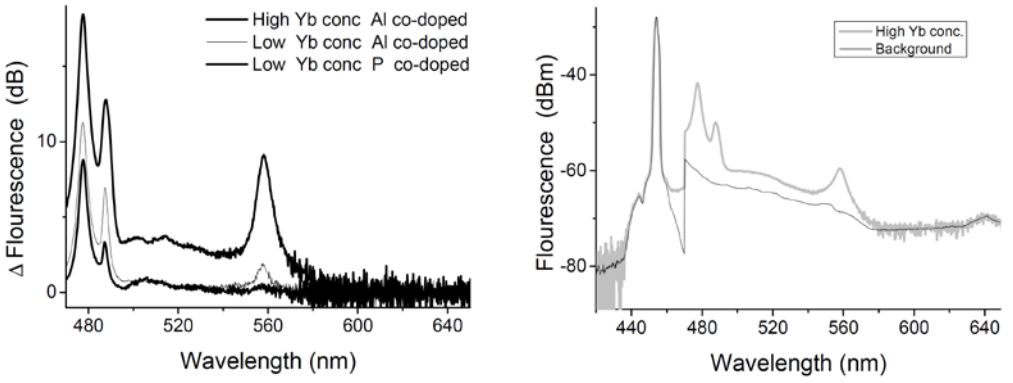

Fig. 5. **a)** Difference luminescence spectra from high Yb concentration (Al co-doped) and low Yb concentration (Al and P co-doped) fibers showing significant difference in 500 - 558 nm luminescence reflecting their difference when inspected by the eye: green for Yb/Al co-doped fibers and blue for Yb/P co-doped fibers, **b)** the high Yb concentration emission and background reference luminescence show identical emission for pump (450–460 nm) and pulling bands (636 nm).

#150869 - $15.00 USD Received 11 Jul 2011; revised 2 Sep 2011; accepted 2 Sep 2011; published 26 Sep 2011

The “remaining” absorption of Yb/P co-doped samples show centers at 3.15 eV (0.35 eV), 2.82 eV (0.70 eV) and 1.55 eV (0.45 eV) as shown in Fig. 4 b). The values in brackets are their respective FWHM.

The luminescence spectra of Yb/Al (high and low Yb concentration) and Yb/P co-doped fibers are nearly identical as shown in Fig. 5 a). To suppress the background luminescence from the pump core the spectra are obtained by subtracting the luminescence measured in an Yb-free fiber with identical mode characteristics operated for 46 hours (without observing any PD). The luminescence of the high Yb concentration fiber is shown (light gray) along with the passive fiber background luminescence (black line) in Fig. 5 b). By subtracting the background luminescence from the measured active fiber luminescence the pump (450–460 nm) line and red luminescence (≈645 nm pulling band) are removed. That the 450 –460 nm was due to the pump was tested by change of pump wavelength to 976 nm where after only this line shifted (to 482 nm). The remaining luminescence spectra in Fig. 5 a) show lines at 477–478 nm, 487–488 nm and 557–559 nm along with a broader spectrum centered at 500–520 nm. The intensity of the various lines scales at different factors to the ytterbium concentration. The 559 nm line of high Yb concentration material (Al co-doped) is reduced and shifted (towards 557 nm) in low Yb concentration fibers (Al co-doped) and is hardly resolvable for P co-doped fibers. Likewise is the broad 507–510 nm line reduced in going from high to low Yb concentration (Al co-doped) and is nearly not resolved for P co-doping. Inspected by the eye during unseeded amplifier operation the luminescence of Al co-doped fibers appears green whereas P co-doped fibers appear blue in good agreement with the recorded luminescence.

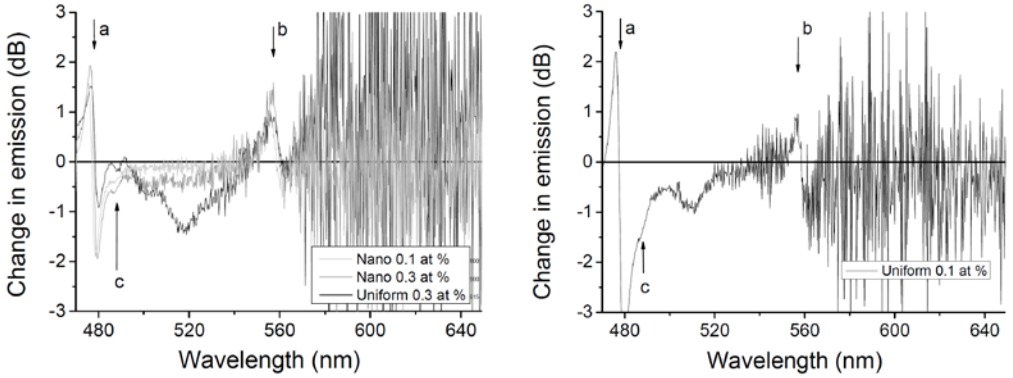

Fig. 6. Difference luminescence spectra after 46 hours PD operation of **a)** two nano-structure (fiber #2 and #3) and one uniform Yb/Al co-doped core fiber (#6) showing growth to peak “a” and “b” while “c” decreases, **b)** one Yb/P co-doped uniform core fiber (#7) showing excess decrease in luminescence at peak “c” which indicates that the pump power may have reduced during PD operation. This is followed by decrease in peak “a” while peak “b” show growth. All spectra are for 46% population inversion.

The luminescence appears constant as function of photo darkening time. However, scaling the spectra at start and after 46 hours to same 530–540 nm level and subtracting these a shift and growth to the peak marked by “a” (477 nm) and growth to the peak marked “b” (558 nm) and decrease for the peak marked “c” (488 nm) for Yb/Al co-doped material is found in Fig. 6 a) for two nano-structure and one uniform core fiber. Here the uniform core fiber in addition to a general decrease in 500 nm–530 nm emission shows a structure of decreased emission around 518 nm. For the Yb/P co-doped uniform core fiber similar behavior is observed in Fig. 6 b) for “b,” “c” and 510 nm emissions while “a” shifts and decreases. The more unstable spectra are found to be a general characteristic of the uniform core fibers. All spectra are of 46% population inversion.

#150869 - $15.00 USD Received 11 Jul 2011; revised 2 Sep 2011; accepted 2 Sep 2011; published 26 Sep 2011

4. Discussion—inter center excited Tm^{3+} luminescence by oxygen deficiency centers

The emission spectra shown in Fig. 5 a) is the result of co-operative emission by two excited Yb^{3+} ions as discussed in [18]. Here the co-operative emission of Yb^{3+} (480 nm–540 nm) is superimposed emission by the rare earth impurities Tm^{3+} ($^1G_4$ for 460 nm–486 nm) and Er^{3+} ($^2H_{11/2}$, $^4S_{3/2}$ in 520 nm - 561 nm). This is taken to show that the co-operative emission by Yb^{3+} pairs is the observed 488 nm line and trace impurities of Tm^{3+} and Er^{3+} are responsible for the 477 nm (2.6 eV) and 558 nm (2.22 eV) emission lines, respectively. The observed difference in co-operative luminescence spectra before and after PD in Fig. 6 are, however, not likely due to increased Yb^{3+} to Tm^{3+} or Er^{3+} excitations in that the optical activity of Yb^{3+} to Yb^{3+} in pairs (co-operative emission at 488 nm) appear to decrease after prolonged PD. A similar decrease in cooperative emission was observed in [19], however, without any change observed for Tm^{3+} or Er^{3+} emission (which may be due to lower amounts of trace impurities for the in [19] applied material compared to the present work). The in Fig. 6 observed relative increase in Tm^{3+}/Er^{3+} luminescence is proposed to be the result of inter center excitation transfer between PD color centers and Tm^{3+}/ Er^{3+}. The choice of scale to 530–540 nm level influences the assessment of relative change (whether or not lines in or decrease relative to their start values) but does not influence the observed relative increase in line “a” 477 nm and “b” 558 nm relative to cooperative Yb^{3+} emission line “c”. The choice of leveling to the 530–540 nm range is justified by the expected relative low probability for either Yb or Er cooperative emission in this range (and hereby expected small change as result of PD).

The data for the uniform core fibers show characteristic structure of decrease at 518 nm (510 nm) for Yb/Al (Yb/P) material while all fibers show uniform decrease in the 500 nm–530 nm emission range in addition to decrease of line “c”. The exact nature of the 518 nm and 510 nm lines of the uniform core fibers are unknown.

In [11] luminescence spectra of Yb/Al co-doped material are given for 250 nm (5 eV) pumping. Here type II oxygen deficiency center (ODC(II)) emission at 4.4 eV is observed along with 2.6 eV / 2.7 eV double peak. Their 2.63 eV emission peak coincide with the in this work suggested Tm^{3+} line while their 2.7 eV peak is ODC(II) as found in [7]. A 2.63 eV emission may be the result of inter center excitation transfer from ODC(II) to trace impurity Tm^{3+} ions. The ODC(II) emission by pumping at 5 eV is in [11] taken to show that ODC(I) converts to ODC(II) which again after prolonged pumping converts to non-bridging oxygen hole centers (NBOHC) in growing emission at 1.91 eV. NBOHC show absorption at 4.8 eV and 2.0 eV where upon excitation into either band emission at 1.91 eV is observed [7]. In the present work no change to 1.91 eV luminescence is observed that can be related to ODC(II) or its conversion. The light observed for this line appears only to relate to the drawing process for the fibers. This difference to [11] could be due to the much higher photon energy applied in this work (5 eV) compared to the present work pumping at 915 nm (1.35 eV).

In [10] thermo stimulated luminescence (TSL) of Yb/Al is found to produce characteristic near-infrared Yb^{3+} emission. This luminescence follows TSL curves as found for Al and Ge co-doped material, which is taken to show that PD induces hole traps in the vicinity of Yb^{3+}. These traps alone cannot account for the PD color center as they are also in Al and Ge co-doped material where PD absorption not is observed.

The two dips that develop over time for Yb/Al co-doped PD absorption spectra marked “a” (2.64 eV–2.58 eV) and “b” (2.22 eV) in Fig. 3 a) coincides with the observed extra emission lines of Tm^{3+} and Er^{3+}. The absorption spectra are for pump switched off recorded by low intensity white light radiation while the luminescence spectra are for pump on. For the analyzing light intensity applied during the measurements no near infrared Yb^{3+} luminescence could be observed initially but after prolonged time a small increase in Yb^{3+} luminescence is detected in line with the observations to line “b” (Er^{3+}). As the pump is switched off during the absorption measurements the observation of luminescence by rare earth ions is taken to show that a by PD induced color center assist the emission. The ODC(II) show 2.7 ± 0.2 eV

#150869 - $15.00 USD Received 11 Jul 2011; revised 2 Sep 2011; accepted 2 Sep 2011; published 26 Sep 2011

luminescence by excitation to its 3.15 ± 0.34 eV absorption center. This is in good agreement with the 3.12 eV–3.15 eV absorption line found by Gaussian center decomposition of the absorption spectra in Fig. 4 b) and correlated growth of 2.6 eV dip in Fig. 4 a). For the "b" dip the observed shallow emission may be due to tails of the ODC(II) emission giving inter center excitation transfer to Er^{3+}. The observed Yb^{3+} emission (at 1.27 eV) must, however, be due to inter center excitation transfer from another part of the PD color center than ODC(II).

The correlated growth of 477 nm emission together with the near infrared Yb^{3+} luminescence by UV [11] and by thermal agitation [10] are taken to show that type I oxygen deficiency ODC(I) (≡Si-Si≡) shown in Fig. 7 a) is a precursor to PD. Here "≡" identifies three Si-O bonds while "-" is the single bond between two silicon. ODC(I) is converted to ODC(II) through PD. The structure for ODC(I) is generally agreed upon while for the diamagnetic character ODC(II) it has proven challenging to find one structure to agree on [7]. Here twofold coordinated silicon =Si: (Silylene or Si_2^0) [20] is opposed a neutral oxygen vacancy (NOV) model (see references in [7]).

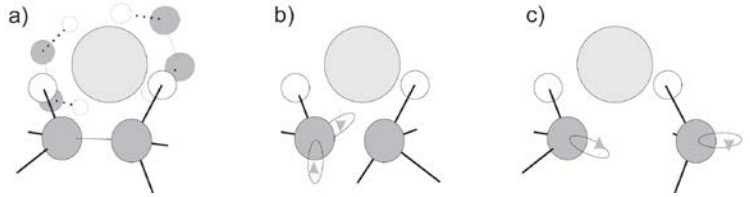

Fig. 7. **a)** An ODC(I) presents two NBO to Yb^{3+} in accommodating part of Yb^{3+} 6-fold coordination to oxygen **b)** two-fold coordinated Si_2^0 model for ODC(II) next to Yb^{3+}, **c)** neutral oxygen vacancy (NOV) model for the ODC(II) precursor where the center silicon is shifted to its un-relaxed (puckered) position.

In Fig. 7 a) is ODC(I) proposed to present two non-bridging oxygen (NBO) to Yb^{3+}. Here Yb^{3+} holds six-fold coordination to oxygen that in [21] is expected to be achieved by edge sharing SiO_4 units presenting two NBOs each. The 50% ionic character of the Si-O bond [22] presents a way to explain the observed coordination in that each Si-O bond demands one "extra" half electron leaving one half electron available in the NBO for coordination against the three valence electrons of Yb^{3+}. By six NBO the +3 valence of Yb is matched. Only NBOs are shown in Fig. 7 a) along with Yb and Si. The conversion to Si_2^0 is in [7] proposed to involve the dissociation of one Si-O bond (demanding ≈5 eV) of ≡Si-Si≡ in forming = Si: and = Si = . This leads to two-fold coordinated silylene Si_2^0 and fully linked SiO_4 as illustrated in Fig. 7 b). The NOV model of ODC(II) precursors is shown in Fig. 7 c). Here the silicon shifts to an intermediate or through its basal oxygen plane to a puckered position leaving lone electrons on either silicon. For the puckered position the lone electron forms a chemical bond to nearby oxygen (neutral three-fold coordinated oxygen) which according to [23] results in optical absorption at 2.8 eV. The ODC(II) absorption at (5 eV / 3.15 eV) and luminescence (2.7 eV) involves the ionizing transfer of an electron in the puckered site while 4.4 eV emission is for the intermediate site by 5 eV absorption. The ionizing transfer of an electron from the puckered site forms positive three-fold coordinated oxygen which is stable but optically inactive at 2.8 eV [23].

Post fiber manufacture processing by oxygen [4] or hydrogen [6] loading are found to reduce PD—i.e. the gaseous species may form bonds to the Si-Si link removing the ODC(II) precursor. The reaction with hydrogen is in [6] found to reduce PD as well as optical activity for Yb^{3+} suggested to be due to Yb^{2+} formation. The reaction with hydrogen might, however, as well be in formation of OH on the six-fold NBO coordination to Yb^{3+} hereby distorting its crystal electrical field and change the optical activity [21]. This comes in addition to beneficial removal of Si-Si bonds. For the present work diminished PD upon H_2 load was observed for Yb/Al material. However, after ≈40 hours pumping by 915 nm radiation growth in PD returns as H_2 diffuses out of the material probably due to release from Si-H H-Si bonds. In this aspect

#150869 - $15.00 USD Received 11 Jul 2011; revised 2 Sep 2011; accepted 2 Sep 2011; published 26 Sep 2011

the oxygen load of [4] look promising (much stronger Si-O bond) but its long term stability is unknown.

In [19] diminished PD is achieved for reducing conditions during pre-form manufacture that, however, also brings reduced optical activity of Yb^{3+}. These observations correspond to the effect of hydrogen loading and stand in contrast to the effect of oxygen loading [4]. The reducing conditions may produce larger concentration of ODC(I) but the concentration of NBO decreases leading to the observed reduced optical activity. In the next section it is proposed that ODC(I) resides on a planar four-fold (or larger) ring and that its conversion into ODC(II) involves a displacive transition. The displacive transition threshold for a four-fold ring is estimated to ≈1.53 eV while the threshold for a three-fold planar ring >5 eV. So if as result of oxygen deficiency the relative concentration of three-fold to four-fold rings increases the number of available precursors to PD decreases (by 1.35–1.27 eV pumps) as is observed in [19].

In [24] it is found that Tm impurities in excess of 10 mol-ppm strongly accelerates PD and increases the total PD loss while Er impurities cause a decrease in PD through decrease in Yb inversion. The amount of impurities are therefore of importance if in excess of 10 mol-ppm. At low Tm^{3+} concentrations, however, the PD behavior of Yb/Al fibers is an intrinsic feature of the material [24] and not caused by Tm^{3+} trace impurities as proposed in [25].

The amount of trace impurities was not determined for the material of the present work, but an estimate is given in the following. The (fiber #3 in [24]) Yb co-doped silica material with 0.08 mol-ppm Tm^{3+} trace impurities shows Tm^{3+} emission intensity ≈6 dB below the cooperative Yb^{3+} emission (488 nm) line while the fibers of the present work show ≈6 dB increased Tm^{3+} intensity relative to 488 nm. The Yb to Al ratio is for both fiber #5 of this work and fiber #3 of [24] in excess of 10 why the relative intensity of 488 nm emission (due to Yb-Yb pairs) is taken to be equal. The difference in Tm^{3+} intensity between the two fibers is a factor of 2^4 why 0.08 mol-ppm Tm^{3+} trace impurity level scales to about 2 mol-ppm trace impurity level for fiber #5 of the present work judging from Tm^{3+} emission intensity as function of concentration presented in [24]. The Er emission intensity found in Fig. 5 is about ≈4 dB below the 488 nm emission intensity why in assuming similar efficiency in transfer to both types of rare earth trace impurity ions the Er trace impurity level is assessed to about half the Tm^{3+} impurity level–i.e. ≈1 mol-ppm. With typical 1–2 mol-ppm up to 10 mol-ppm Tm^{3+} for the highest Yb concentration samples (fiber #1 and #2) the level for trace impurities hold according to [24] no significant influence on the equilibrium PD levels. In the following both Tm^{3+} and Er^{3+} are considered to play a structural role identical to Yb^{3+}.

5. Discussion—Low energy formation of ODC(II) near Yb^{3+}

The formation of ODC(II) is in [10] found to be achieved by ≈2.5 eV radiation in material co-doped with Yb^{3+} in contrast to similar material without Yb^{3+} doping that only shows ODC(II) formation upon 5–6 eV radiation. The latter observation is as would be expected from the ODC(II) models of section 4) while ODC(II) formation by 2.5 eV radiation is unexpected—unless it is due to two-photon excitation processes as proposed in [10]. In the present work the PD is observed upon 1.35 eV pumping as it is in [1–3,5] which, however, may be due to co-operative emission by Yb^{3+} pairs or to Yb^{3+} to Tm^{3+}/Er^{3+} trace impurities delivering 2.6 / 2.2 eV for initiation of the PD process.

In [26] is the NOV model to an ODC(II) precursor found to demand 0.5 eV in activation energy with ≈1.5 eV raise to structural energy for the transition to the puckered position in a two ring cluster (emulating α-quartz structure). The reverse process shows equal 0.5 eV in activation energy. This suggest that the structural transition from ODC(I) to ODC(II) may be achieved by ≈2 eV while the opposite transition demands only 0.5 eV in a bi-stable process. The NOV model anticipates that a slightly soft Si-Si bond has formed for the puckered position facilitating 5 eV ionization to open its ODC(II) response.

#150869 - $15.00 USD Received 11 Jul 2011; revised 2 Sep 2011; accepted 2 Sep 2011; published 26 Sep 2011

By applying displacive transitions an estimate for structural energy is found in assuming that the ODC(I) reside on a planar silica ring. Here it presents two NBOs to adjacent Yb^{3+} as illustrated in Fig. 8 a) for a four-fold ring. In the four-fold ring its common 160° ≡Si-O-Si≡ bridge angle [27] is altered to 166° to accommodate ODC(I) in 246 pm Si-Si bond length [26]. In Fig. 8 b) is the effect of a violet displacive agitation shown where the ≡Si-O-Si≡ bridge angles of the ring has changed to 130°. The energy require for this change may find an estimate from [27] in ≈0.17 eV/bridge angle. The 3 bridges of the ring added the 6 connecting bridges lead to ≈1.53 eV for the transition in fair agreement with the findings for the NOV model. Hereto is to be added the strain to the next layer of connecting SiO_4 tetrahedral units to the defect ring. A large part of this strain is only temporal and will be released upon return to the equilibrium structure (within ≈1 ps corresponding to two periods of the 440 cm^{-1} network phonon angular rotation).

The displacive transition of Fig. 8 b) is performed with fixed silicon centers while the bridging oxygen is displaced (as indicated by the arrows). Such a displacive transition will for the two three-fold coordinated units translate into strain on their Si-Si bond and rotation around the bridging oxygen (outside the plane of the ring) as indicated in Fig. 8 b) by the curved arrows. Dependent on the angle of rotation around the oxygen outside the ring this may bring one of the neighbor NBOs close (within a Si-O bond length) to the strained Si-Si bond as shown in Fig. 8 c).

In [28] it is proposed that the paramagnetic center of silica NBO (Si-O·) is a deep electron traps that is able to form stable negatively charged centers. It is found that the negatively charged NBO^- (Si-O:) show adiabatic electron affinity of 5.3–5.8 eV while the E' center

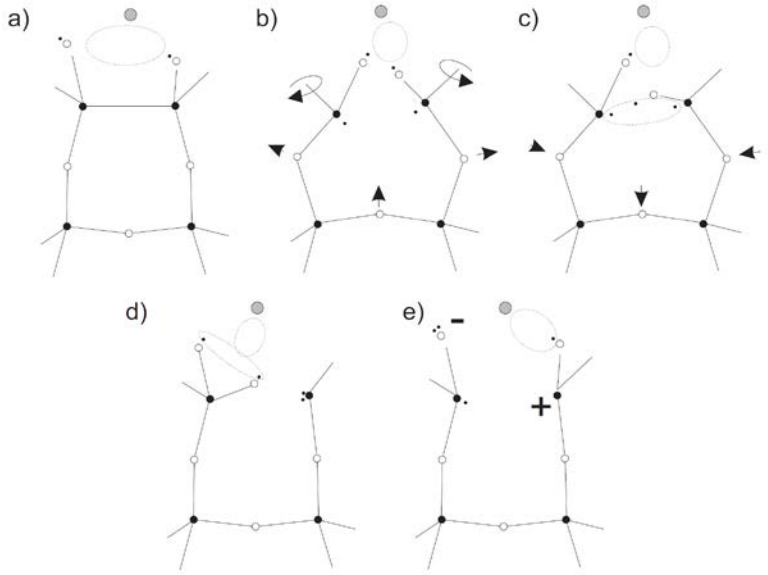

Fig. 8. **a)** A four-fold defect ring accommodates ODC(I) adjacent to Yb^{3+} (shown at the top with its valence electron bond indicated by the dotted ellipse), only silicon and bridging oxygen of the ring are shown along with two NBOs presented to Yb^{3+}, **b)** Vigorous displacive transition shifts the position of oxygen (indicated by arrows) while the silicon remain in fixed positions—except for the two three-fold coordinated units where rotations around the out of plane bridging oxygen (indicated by curved arrows) lead to shift in both NBOs and silicon centers, **c)** one NBO moves into the vicinity of the strained Si··Si bond, that assisted by structural relaxation and by photon excitation in a **d)** charge disproportionation process results in a Si_2^0 center next to a fully linked dioxasilirane (= $Si<O_2$) through NBO transfer **e)** ≡Si^+ hole trap opposed NBO^- electron trap in charge disproportionation process final step prior to ODC(II) formation.

#150869 - $15.00 USD Received 11 Jul 2011; revised 2 Sep 2011; accepted 2 Sep 2011; published 26 Sep 2011

precursor (≡Si··Si≡) shows 7.3 - 7.7 eV vertical ionization potential. The net cost for a charge disproportionation process in: ≡Si· + ≡Si-O· → ≡Si^+ + ≡Si-O^- is ≈1.57 eV for β-cristobalite and ≈1.92 eV for α-quartz.

Here it is proposed that a charge disproportionation process transforms the strained ≡Si-Si≡ bond into = (Si^+)-O^- + ≡Si· in that the charge transfer goes between host silicon and its NBO. This process may in a following relaxation lead to transfer of the NBO to the next neighbor as shown in Fig. 8 d) leading to Si_2^0 and dioxasilirane formation. This transition takes place if a dative bond forms between the NBO^- and its neighbor silicon where the formation energy of this bond together with charge relaxation in return of the electron to Si^+ supplies sufficient potential energy to dissociate the old Si-O bond. This will leave a two-fold coordinated silicon (silylene) next to dioxasilirane.

The charge disproportionation process may also result in = Si^+ + ≡Si-O^- in that charge transfer goes between a silicon and its next neighbor NBO. The second process will in relaxation lead to ODC(II) of the NOV model as shown in Fig. 8 e). The charge relaxation in forming ≡Si: is possible in that the ≡Si: and ≡Si-O: electron traps are almost equal in trapping potential. Here ODC(I) show 7 eV ionization potential while ODC(II) show about 5 eV while the charge disproportionation process demands 1.6–1.9 eV. I. e. the transfer of one electron from ≡Si-O: to ≡Si· (in forming ≡Si:) must demand ≈0.5 eV which may be supplied in the relaxation of structural strain on reversing the displacive transition which initiates ≈0.5 ps after the last excitation.

The draw on excitation energy for the charge disproportionation process may be reduced through the presence of the NBO to the Si-Si why it is taken to supply ≈0.7 eV FWHM to the 1.6–1.9 eV in excitation energy giving high probability for pump photons to initiate the process. The FWHM of the process is taken to be about half the electron affinity of atomic oxygen.

The disproportionation process between host silicon and its NBO may be the very process that initiates the displacive transition. Here excited Yb^{3+} may lead to displacement of one NBO against its host giving raise to the process. This would suggest that initially the excited Yb^{3+} opens an unstable color center which relaxes into displacive transitions. The induced displacive transition will reverse within ≈1 ps and the possible new coordination relaxes into a ODC(II) structure with practically no remaining strain as may be taken from Fig. 8 d) and e).

6. Discussion—UV absorption and oxygen centers

Resemblance between the PD color center and ozone absorption tails (in the visible and near infrared) is found for the Yb/Al co-doped material as shown in Fig. 2. If this resemblance is to be taken to be due to presence of gaseous ozone [29] produced during PD this is followed by 254 nm (4.88 ± 0.74 eV peak of Hartley band) absorption [17]. The in [4] observed reduction in PD by O_2 loading goes, however, against this proposal and renders it unlikely that ozone plays a role for PD. The formation of ODC(II) centers in the NOV model on the other hand is from section 5 expected to be followed by ≈5 eV (4.99–4.93 eV) absorption or alternatively dioxasilirane combined with silylene.

In [11] growth in absorption from below 230 nm (>5.4 eV) to 257 nm (4.82 eV) is recorded for 250 nm radiation of Yb/Al co-doped samples. The observed peak absorption at 248 nm (5.0 eV) is assigned to growth of ODC(II) while growth in >5.4 eV absorption is assigned to ODC → E' conversion. The latter agrees with [4] where absorption at 220 nm (≈5.63 eV) is assigned E' centers observed upon 488 nm radiation of Yb/Al co-doped samples. However [5], reports intermediate ≈230 nm (5.4 eV) absorption due to charge transfer bands in Yb^{2+} formation by trapping holes on ligand oxygen. These can, however, from Fig. 2 in [5] be observed to yield maximum (976 nm) luminescence intensity for 220 nm excitation. As the effect of Yb^{2+} not could be reproduced experimentally in [19] the nature of the ≈230 nm band may need further consideration.

#150869 - $15.00 USD Received 11 Jul 2011; revised 2 Sep 2011; accepted 2 Sep 2011; published 26 Sep 2011

In [30] a surface defect pair that consists of dioxasilirane and silylene yield 5.4 eV absorption resulting in fluorescence at 3.7 eV. In [31] surface dioxasilirane is found to show (5.63 eV) absorption without fluorescence. Here (5.63 eV) absorption by dioxasilirane reads on the measurements by [4] and the accompanying Si_2^0 center (5 eV) reads on [11] while combined [30] they read on [5]. So dioxasilirane and silylene in various combinations may cover the observed range of measurements on various Yb/Al co-doped silica fibers of different origin (most processes are only partly disclosed).

In the present model of the color center the valence electron of ytterbium is intimate related to the dioxasilirane in forming a highly ionic character bond. This leads to that the two-fold coordinated silicon attached oxygen molecule practically is to be considered a super oxide. The (0.43 eV) electron affinity of molecular oxygen [32] that follows creation of super oxide may, however, indicate that this compound is relative unstable why deionization of the super oxide in return to dioxasilirane easily is achieved. The super oxide of Alkali Halide crystals shows 5 ± 1 eV absorption with fluorescence in the 2.1–2.5 eV [33].

In the NOV model picture the 5 eV absorption is delivered directly from ODC(II) while the conversion of ODC(II) to E' centers may cover the observations by [4] and [11]. No directions are available to [5] with observation of Yb^{3+} luminescence upon excitation in the 5.4 eV band.

7. Discussion—PD color center absorption and oxygen centers

The observed absorption spectra in Fig. 4 b) of Al and P co-doped material are in this section explained in the context of the two possible versions of color centers found in section 5.

For the NOV ODC(II) the observation has to rely on that ODC(II) of NOV actually give raise to the expected absorption / emissions but these may be found as for silylene [7]. The infrared and visible part of the spectrum lacks, however, in that the electron on ≡Si: against the lower potential energy ≡Si-O: electron trap (according to the considerations in section 5) not is expected to give absorption in the visible / near infrared. However, if a "silent population" of NOV centers are available the charge disproportionation process from ≡Si· to ≡Si-O: may result in absorption for the 1.6–1.9 eV range in 0.7 eV FWHM.

In the silylene/ dioxasilirane model the ≈3.15 eV and ≈2.8 eV absorptions are due to silylene in phonon assisted and zero-phonon absorptions, respectively [20]. Dioxasilirane does not appear to give away any absorption in the visible or near infrared but is expected together with the valence electron of Yb^{3+} to form super oxide. However, the stability of this bond is relative low why a near-infrared "silent" population of color centers may exist as in the case of the NOV model if the bonding electron of the three-electron bond is captured by either of the NBO electron traps in its vicinity.

For the visible and near infrared the super oxide model may be taken to follow the absorption of molecular super oxide. From the spectroscopic data of [32] the paramagnetic super oxide is found with $X^2\Pi_g$ ground state and three excited states $^4\Sigma_u^-$, $^2\Pi_u$ and $^2\Sigma_u^-$. The anion molecule is taken to hold "1½" bond characteristics in its ground state and first two excited states while the third excited state show a "½" bond. The bonds of these four states may by applying the Morse potential function be described by the bond dissociation energies and (bond length) as: 4.07 eV (133 pm), 1.502 eV (163 pm), 0.61 eV (163 pm) and 0.093 eV (175 pm), respectively. The three excited states bond length fits the inter oxygen $Si<(O)_2$ bond length of ≈161 pm in 110° O-Si-O angle of dioxasilirane [31].

The excited states of the super oxide involving "1½" bonds are accommodated as anion dioxasilirane by traditional linking to silicon where the (two) oxygen donates one electron in return of 50% ionic character to their bonds [22]. This is illustrated by three-electron bonds assigned to Si-O in Fig. 9 a). The "extra" electron in bond with Yb^{3+} is accommodated in the three electron bond next to the σ-bond linking the oxygen in Fig. 9 a). This three-electron bond is in molecular orbital calculations regarded to comprise two bonding electrons and one anti-bonding electron which, however, in [34] is shown to be equal to two parallel spin

#150869 - $15.00 USD Received 11 Jul 2011; revised 2 Sep 2011; accepted 2 Sep 2011; published 26 Sep 2011

electrons residing on each atom with one bonding electron between as applied in Fig. 9. For the third excited state of the super oxide only the three-electron bond links the oxygen as shown in Fig. 9 b) while the ionic character of the Si-O bonds is reduced (as discussed in the following).

The spectroscopic data for super oxide [32] is shown in Fig. 9 c) by the solid dots while their Morse potential function fits are given in the solid curves. The dotted curves are the six stable states of molecular oxygen O_2 fitted by a Morse potential function. It is here noted that by applying the electron affinity of atomic oxygen for the super oxide in reflection of the added shield by one extra electron the atomic oxygen electron affinity fits the spectral data.

From Fig. 9 c) the three excited state of super oxide is expected to show 2.98 eV, 2.09 eV and 1.57 eV absorptions in excitation of the electron against Yb^{3+} for the proposed working model of the color center. The absorption by 2.98 eV may in combination with silylene absorption at 3.15 eV give raise to the observed shift in peak absorption for the Al co-doped spectrum of Fig. 4 b). The 2.09 eV is to correspond to the "ozone" absorption while 1.57 eV is to match the 1.55 eV applied in the Gaussian center de-composition of the absorption spectrum. The 133 pm bond ground state of super oxide would give rise to ≈5.56 eV (222 nm) absorption which actually is close to the measured 5.63 eV (220 nm) of dioxasilirane [31].

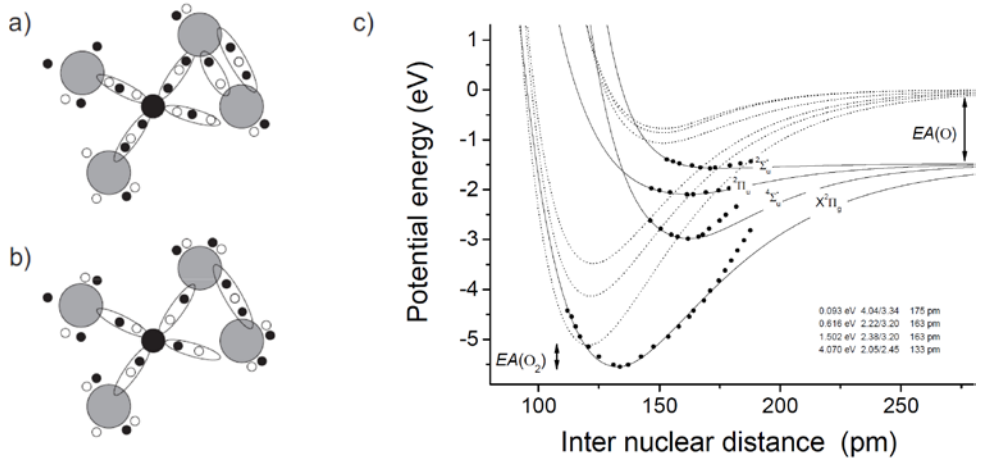

Fig. 9. **a)** Anion dioxasilirane forms "1½" superoxide bond between oxygen, the open and closed dots are electrons of opposite spin while the black center is silicon surrounded by four oxygen, **b)** Anion dioxasilirane forms "½" superoxide bond, **c)** potential energy for four stable states of super oxide from [32] (dots) fitted by solid lines (Morse potential curves) while the dotted lines are Morse potential curves for the six stable states of molecular oxygen O_2 fitted to data by [32]. By applying the electron affinity of atomic oxygen the experimental electron affinity of O_2 fits the data as indicated.

The difference in absorption spectra observed from Fig. 4 b) in going from Al to P co-doping may be described as a shift from "1½" bond dominance to "½" bond dominance of the anion dioxasilirane. This leads in the visible to 1.57 eV dominance over 2.09 eV while the phonon assisted absorption by silylene dominates in the blue part due to reduced "1½" bond anion dioxasilirane character. This may be taken to indicate that the ionic character of the Si-O bonds have decreased for phosphorous replacing aluminum co-doping.

The decrease in ionic character of Si-O bonds may indicate that the acidity of the glass material changes with change of co-doping. Here acidity is generated through difference in electrostatic potential of the substitute co-doping elements [35]. Here a cation inserted into SiO4 in replacing Si will if it experiences more negative potential accept electrons more readily. The cation will act as a new Lewis acid site. Aluminum shows lower (Pauling) electro negativity than Si that again shows less negativity than P. I. e. in relation to Al co-doping Si can accept electrons more readily than in relation to P co-doping. This is taken to indicate that

#150869 - $15.00 USD Received 11 Jul 2011; revised 2 Sep 2011; accepted 2 Sep 2011; published 26 Sep 2011

the Si-O bonds of dioxasilirane reduce in ionic character for increased P co-doping. This again gives cause to the reduced order in chemical bond observed in the dioxasilirane.

Judging only from Pauling electro negativity other interesting co-doping atoms may be anticipated to give raise to decreased Lewis acidity in that Al < Si < Ge < B < P. Here, however, a replacement of Si by Ge leads to considerable higher PD than observed for Al co-doping [36]. So, in addition to the acidic response of Al versus P it is to be taken into account that these two elements form solvation shells to rare earth elements [37,38] in contrast to Ge and B. For Ge co-doping the not forming solvation shells is indirectly assessed from the requirement of co-doping with Al to avoid clustering [39] while it is directly observed for boron in [38].

Without solvation shells the incorporation of rare earth elements still takes place through ODC(I) formation but without the beneficial effect of reducing the number of Yb-Yb ion pairs. Further will the absence of a solvation shell infer that the "1½" bond on dioxasilirane dominates judging from the absorption spectra of Ge co-doped material to be found in [36]. I. e. both presence of solvation shell and low Lewis acidity of the shell is required to reduce the color center to "½" bond and the herewith beneficial effect in the near infrared on the absorption spectrum.

Taking solid acidity as a measure for the ionic character of the dioxasilirane bonds the Lewis acidity of aluminum co-doped silica is higher relative to phosphorous co-doped silica [35]. This change in acidity by co-doping may also be the reason for the observed beneficial effect of adding cerium to Yb/Al co-doped material [15]. Here CeO_2 show lower acidity at its surface than Al_2O_3 [35].

8. Conclusion

The photo darkening (PD) absorption spectra from unseeded amplifier operation (by 915 nm pumping) of ytterbium / aluminum and co-doped silica fibers is after prolonged operation observed to develop a characteristic line at 2.6 eV (477 nm) along with a 2.2 eV (558 nm) dent. These two lines is proposed to be due to inter center excitation transfer from type II oxygen deficiency center ODC(II) to Tm^{3+} and Er^{3+} trace impurities, respectively.

The precursors for ODC(II) are type I oxygen deficiency centers ODC(I) found at the interface between Yb/Al clusters and the surrounding silica network. The six-fold coordinated Yb^{3+} (and Al^{3+}) cluster is proposed to be linked into the silica glass network through pairs of non-bridging oxygen (NBO) some of which resides on ODC(I) with one NBO attached to each of the three-fold coordinated silicon units. Each pair of NBO supply a bond site for one (of three) valence electrons of Yb^{3+}.

The actual structure of ODC(II) is not resolved why two alternative structure models for the PD color center are proposed based on two contemporary models for ODC(II). Here the color center based on silylene (two-fold silicon unit with one electron pair) combined with anion dioxasilirane (two-fold silicon with a super oxide molecule attached) is found to yield the best fit to observations made in this work along with observations presented by reference.

It is proposed that the PD process goes in consecutive excitations by pump photons following each other with not more than 0.5–1 ps between excitations. Here the action of three pump photons is taken to deliver sufficient energy to create a color center through a displacive transition of a 4-fold (or larger) silica ring hosting ODC(I) precursors. The displacive transition is initiated by a charge disproportionation process which in two rounds leads to NBO transfer in forming dioxasilirane. This center may, however, be silent in that a fraction of the created color centers are expected to show uneven charge distribution on dioxasilirane preventing the formation of three-electron chemical bonds.

Difference in solid acidity of silica material co-doped with Yb/Al and Yb/P that both form solvation shells to rare earth elements may explain their observed difference in spectral shapes by change in bond order to the formed chemical bond of dioxasilirane.

#150869 - $15.00 USD Received 11 Jul 2011; revised 2 Sep 2011; accepted 2 Sep 2011; published 26 Sep 2011

Acknowledgment

The financial support from the Leadership in Fiber Laser Technology (LIFT) project under the 7th Framework Program of the European Commission is acknowledged.

#150869 - $15.00 USD Received 11 Jul 2011; revised 2 Sep 2011; accepted 2 Sep 2011; published 26 Sep 2011